Neurospine 2022;19(3):828-837.
https://doi.org/10.14245/ns.2244146.073

Neurospine
pISSN 2586-6583 eISSN 2586-6591

Original Article

# Biomechanical Effects of Proximal Polyetheretherketone Rod Extension on the Upper Instrumented and Adjacent Levels in a Human Long-Segment Construct: A Cadaveric Model

**Corresponding Author**
Brian P. Kelly
https://orcid.org/0000-0002-5551-2834

c/o Neuroscience Publications; Barrow Neurological Institute, St. Joseph's Hospital and Medical Center
350 W. Thomas Rd.; Phoenix, AZ 85013, USA
Email: Neuropub@barrowneuro.org

Received: February 22, 2022
Revised: May 11, 2022
Accepted: June 12, 2022

Bernardo de Andrada Pereira[1], Jennifer N. Lehrman[1], Anna G.U. Sawa[1], Piyanat Wangsawatwong[1], Jakub Godzik[2], David S. Xu[2], Jay D. Turner[2], Brian P. Kelly[1], Juan S. Uribe[2]

[1]Spinal Biomechanics Laboratory, Barrow Neurological Institute, St. Joseph's Hospital and Medical Center, Phoenix, AZ, USA
[2]Department of Neurosurgery, Barrow Neurological Institute, St. Joseph's Hospital and Medical Center, Phoenix, AZ, USA

**Objective:** The high mechanical stress zone at the sudden transition from a rigid to flexible region is involved in proximal junctional kyphosis (PJK) physiopathology. We evaluated the biomechanical performance of polyetheretherketone (PEEK) rods used as a nontraditional long semirigid transition phase from a long-segment metallic rod construct to the nonfused thoracic spine.
**Methods:** Pure moment range of motion (ROM) tests (7.5 Nm) were performed on 7 cadaveric spine segments followed by compression (200 N). Specimens were tested in the following conditions: (1) intact; (2) T10-pelvis pedicle screws and rods (PSRs); and (3) extending the proximal construct to T6 using PEEK rods (PSR+PEEK). T10–11 rod strain, T9 anterolateral bone strain, and T10 screw bending moments were analyzed.
**Results:** At the upper instrumented vertebra (UIV)+1, PSR+PEEK versus PSR significantly decreased ROM in flexion (115%, $p = 0.02$), extension (104%, $p = 0.003$), left lateral bending (46%, $p = 0.02$), and right lateral bending (63%, $p = 0.008$). Also, at UIV+1, PSR+PEEK versus intact significantly decreased ROM in flexion (111%, $p = 0.01$) and extension (105%, $p = 0.003$). The UIV+1 anterior column bone strain was significantly reduced with PSR+PEEK versus PSR during right lateral bending ($p = 0.02$). Rod strain polarities reversed with PEEK rods in all loading directions except compression.
**Conclusion:** Extending a long-segment construct using PEEK rods caused a decrease in adjacent-level hypermobility as a consequence of long-segment immobilization and also redistributed the strain on the UIV and adjacent levels, which might contribute to PJK physiopathology. Further studies are necessary to observe the clinical outcomes of this technique.

**Keywords:** Biomechanical phenomena, Bone malalignment, Kyphosis, Polyetheretherketone, Mechanical stress



## INTRODUCTION

Biomechanical understanding of long-segment fusion for adult spinal deformity has progressed in recent years; nevertheless, proximal junctional kyphosis (PJK) remains an unresolved complication of this procedure. The term PJK is used broadly to define clinical observations ranging from loss of alignment to compression fracture and junctional mechanical failure above an upper instrumented vertebra (UIV).[1] PJK is a potential cause of fixation failure (i.e., top screw loosening and pullout)

and consequently an important factor contributing to high rates of revision surgery.[2] Increasing the durability of multilevel constructs and preventing PJK remains challenging and has been the focus of extensive research efforts.

The elasticity modulus of metallic spinal rods (i.e., titanium or cobalt-chrome) commonly used for fusion procedures is much greater than that of tissue, including bone, and this difference in elasticity may significantly alter the distribution of load along the anterior and posterior vertebral columns at the instrumented and adjacent levels during physiologic loading.[3] The high mechanical stress zone created directly above the UIV by the sudden transition from an instrumented rigid to a native flexible region has been hypothesized to be one of the most important factors in the physiopathology of PJK.[4] The occurrence of PJK is notable in the lower thoracic spine, which acts as a fulcrum subjected to high physiological forces created by the passage of lumbar lordotic to thoracic kyphotic curvature—a region under constant gravitational influence of upper body weight. Most strategies described to attenuate this blunt transition consist of creating an intermediate semirigid bridge connecting the 2 very distinct mechanical regions. Previously reported techniques include hooks, posterior bands or ligament augmentation, or cement augmentation, with variable results.[5-11]

Polyetheretherketone (PEEK) rods have been used as a biomaterial in various configurations for semirigid and dynamic stabilization spinal procedures.[12] PEEK is a thermoplastic, biocompatible, radiolucent polymer that resists chemical and radiation damage and that has less rigidity than metallic rods; thus, it has an elasticity modulus that is closer to cancellous bone.[13]

Traditionally, titanium and cobalt-chrome alloys have been used as materials for pedicle screw and rod (PSR) instrumentation. Several laboratory studies have compared PEEK and metallic rod mobility for index-level stabilization, but they have not looked to adjacent-level behavior.[4,14,15] The biomechanical performance of PEEK rods used as a semirigid transition from a long-segment metallic rod construct spanning from the lumbar region to the nonfused thoracic spine has not been studied *in vitro*, to our knowledge. Theoretically, flexible PEEK rods connected immediately above the UIV have the potential to create a more evenly distributed load across columns and thus provide a softer transition that may protect the adjacent spinal level from high mechanical stress. This cadaveric study observed the UIV and adjacent-level range of motion (ROM) and strain distribution (posterior rod and anterior column bone) to investigate how this strategy might help to mitigate PJK occurrence.

## MATERIALS AND METHODS

Seven fresh-frozen human T2-pelvis cadaveric specimens with intact rib cages were selected for this study; 2 were female and 5 were male, with a mean (standard deviation [SD]) age of 60.7 (4.9) years. Medical records and plain film radiographs were reviewed, and direct manual inspection was performed to ensure no obvious pathology was present that might affect the study results. Dual-energy x-ray absorptiometry scans were performed on L4 of each specimen to assess bone mineral density, and the mean (SD) was 0.91 (0.16) g/cm$^2$. Informed consent for this study was not required, and institutional review board approval was not sought because of the cadaveric nature of the investigation.

Specimens were stored at -20°C until test day and then thawed in normal saline at 21°C. Muscles and soft tissues were removed while keeping intact all ligaments, joint capsules, and intervertebral discs. The main rib cage structure was entirely preserved below the second rib; specifically, the intercostal musculature, costovertebral joints, costal cartilage, body of sternum, and xiphoid process were preserved. The first rib and manubrium were removed. The ischium was bilaterally reinforced with household wood screws, placed in a rectangular metallic mold, and embedded using fast-curing resin (Smooth-Cast, Smooth-On, Inc., Easton, PA, USA) to permit attachment to the base of the testing apparatus. The top vertebra (T2) was also reinforced with household screws and embedded in the same resin in a cylindrical-shaped pot for test frame attachment and loading.

### 1. Instrumentation

All specimens were initially tested intact before undergoing PSR fixation. The PSR condition comprised insertion of polyaxial pedicle screws (6.5×45 mm, CD Horizon, Medtronic, Dublin, Ireland) from T10 to S1 and S2 alar-iliac screws (8.5×80 mm, CD Horizon) placed under fluoroscopy guidance (Fig. 1A). Two 5.5-mm diameter cobalt-chrome rods (NuVasive, San Diego, CA, USA) were contoured bilaterally to fit screw heads from T10 to S2 to minimize the need for reduction. After specimens were tested in the PSR condition, the PSR+PEEK condition was tested. The PSR+PEEK condition comprised additional pedicle screws (6.5×45 mm, CD Horizon) that were inserted bilaterally at T6, and the upper instrumented level of the construct (T10) was extended to this level using PEEK rods (6.35×120 mm, CD Horizon) connected to the primary construct using inline axial connectors (Fig. 1B).

PJK revision for constructs with T10 UIV often involves con-

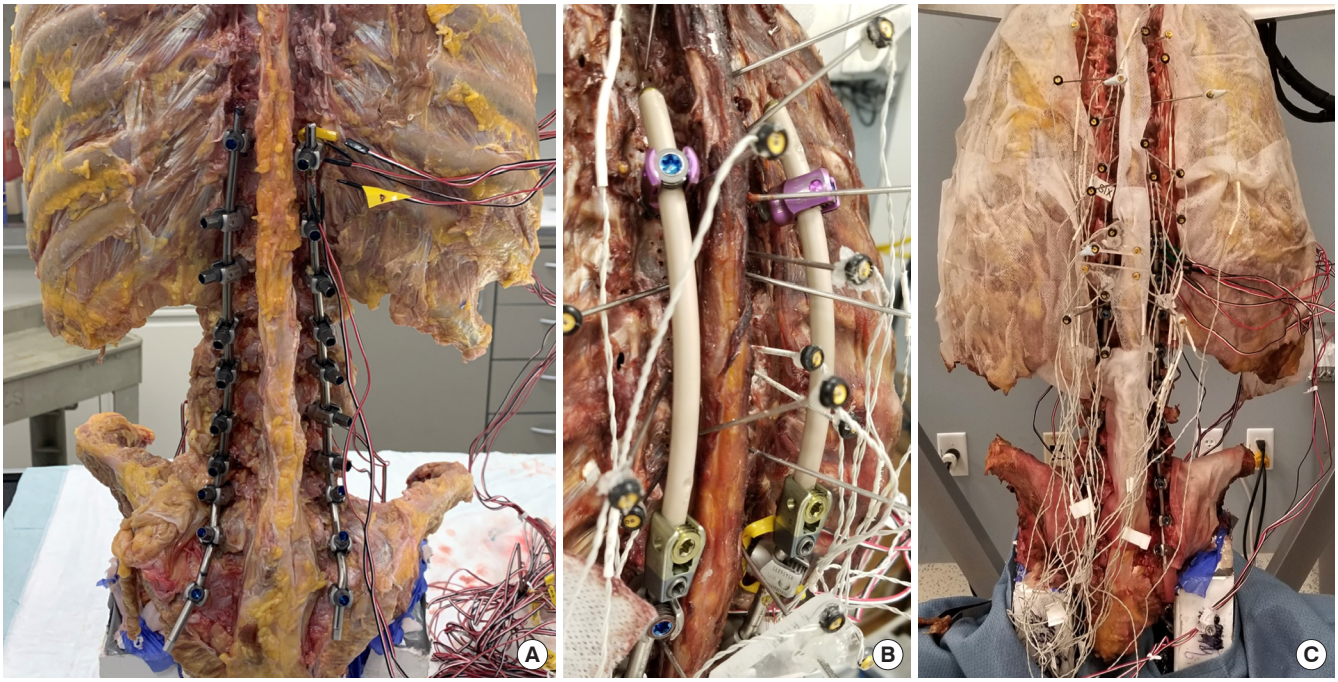


Fig. 1. (A) T10–S2 alar-iliac pedicle screw and rod construct. (B) Polyetheretherketone rods attached with connectors. (C) Specimen on robotic test frame. Adapted with permission from Barrow Neurological Institute, Phoenix, Arizona.

struct extension to T6, while current posterior tension band techniques similarly aimed at offsetting PJK often extend fixation 2 levels above the UIV. Thus, the rationale for investigating a nontraditional extension to T6 was that PEEK rods and screws (T6) could be placed percutaneously, maintain the posterior tension band, and thereby move ahead of T10 PJK by providing a well-distributed "soft landing" above the UIV.

### 2. Biomechanical Tests

Test specimens were fixed caudally to the testing frame table to permit unconstrained relative medial-lateral translation between ilia, and they were fixed cranially to the end effector of a 6-degree-of-freedom robotically controlled test frame[16] (Fig. 1C). For each condition tested (Fig. 2), specimens underwent dynamic nondestructive pure moment flexibility tests of 7.5 Nm at a mean global rotation rate of approximately 1.5° per second for the following motions: flexion, extension, right and left lateral bending, and right and left axial rotation, followed by a vertical compression of 200 N. ROM stability, anterior column bone strain, rod strain, and screw bending moments were assessed for all conditions.

### 3. Angular Motion Tracking

Angular ROM was obtained from 3-dimensional motion measurement with the Optotrak 3020 camera apparatus (Northern

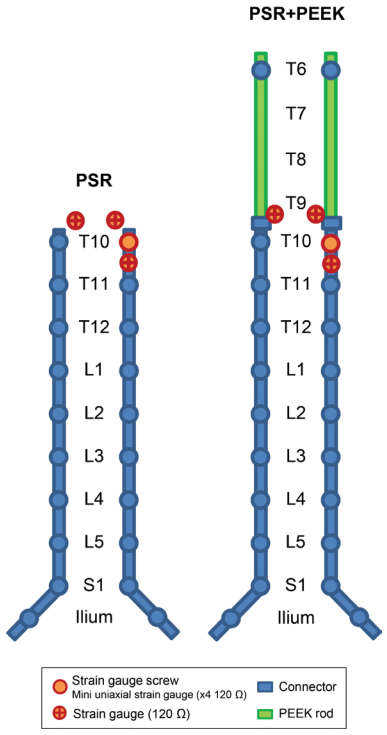


Fig. 2. Illustration showing instrumentation for test conditions. PEEK, polyetheretherketone; PSR, pedicle screw and rod. Adapted with permission from Barrow Neurological Institute, Phoenix, Arizona.


https://doi.org/10.14245/ns.2244146.073

Digital, Waterloo, Ontario, Canada). This system measured stereophotogrammetrically the 3-dimensional motion of infrared-emitting markers attached in a noncollinear arrangement to each vertebra. Custom software was used to convert the marker coordinates to angles about each of the anatomical axes.[17]

**4. Anterior Column Bone Strain**

Each specimen was instrumented with a stacked rosette strain gauge (C2A-06-G1350-120, Micro-Measurements, Raleigh, NC, USA) placed on the left anterolateral surface of the anterior column of the T9 vertebral body (Fig. 3). Principal T9 bone strains during loading in each direction were calculated from strains recorded at 10 Hz using a StrainSmart data acquisition system (Vishay, Micro-Measurements, Raleigh, NC, USA).

**5. Screw Bending Moment and Rod Strain Monitoring**

Before being inserted into bone, the T10 screws on the right side of the specimen were instrumented with 4 circumferentially placed uniaxial strain gauges (C2A-06-015LW-120, Micro-Measurements). A loading calibration procedure was performed on each screw before insertion to establish a strain versus screw bending moment relationship.[18] The right-side rod was instrumented posteriorly with a stacked rosette strain gauge (C2A-06-G1350-120, Micro-Measurements) midway between T10 and T11. The rod gauge was attached after rod contouring, and the instrumented rod was not calibrated before use. Rod and screw strain gauge placements are illustrated schematically in Fig. 2. Rod and screw strains were recorded simultaneously with the bone strains using the same data acquisition system.

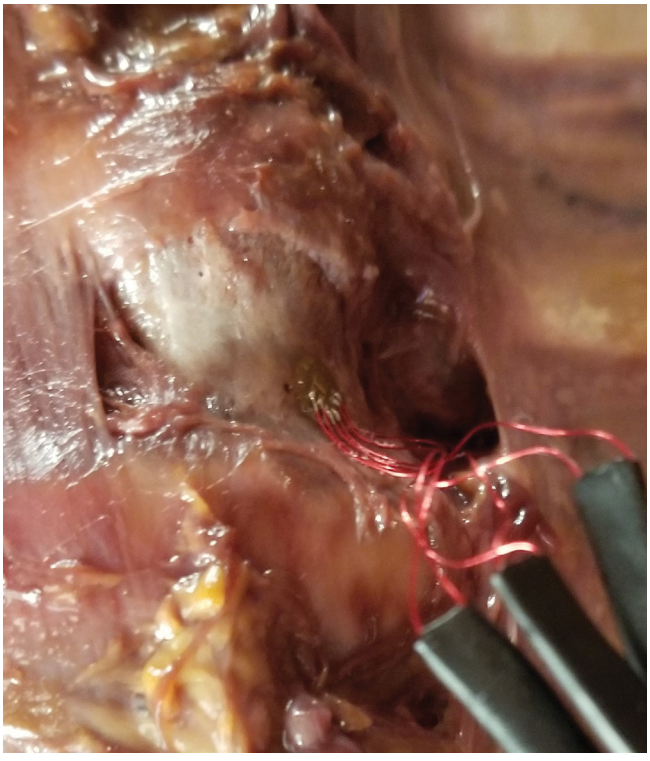

**Fig. 3.** Strain gauge attached to the anterolateral vertebral body surface, left anterior column bone. Adapted with permission from Barrow Neurological Institute, Phoenix, Arizona.

**6. Statistical Analysis**

Statistical comparisons of ROM among conditions (intact, PSR, and PSR+PEEK) were assessed using a one-way repeated-measures analysis of variance followed by Holm-Šidák post hoc comparisons as needed, using an alpha level of $p = 0.05$ (SigmaStat, Systat Software, San Jose, CA, USA). Screw bending moments and bone and rod strains (PSR vs. PSR+PEEK) were analyzed using paired t-tests (Excel, Microsoft, Redmond, WA, USA).

## RESULTS

Overall results showed no obvious evidence of screw or instrumentation loosening, pull out, or failure.

**1. Range of Motion**

ROM values are summarized in Table 1, and all p-values comparing ROM for PSR and PSR+PEEK conditions are summarized in Table 2.

***1) Upper instrumented level (T10–11) ROM***

Compared to the intact condition, PSR instrumentation decreased ROM at the uppermost instrumented level (T10–11) in all loading directions (mean 80%); however, the decrease was only statistically significant during flexion (70%, $p = 0.003$). When extending the PSR construct with PEEK rods, no significant difference was noted between PSR and PSR+PEEK ($p \geq 0.06$). Compared to the intact condition, the PSR+PEEK condition showed a decrease in ROM in all directions of pure moment loads with a mean decrease of 89% and statistical significance in flexion (91%, $p = 0.001$), extension (96%, $p = 0.047$), and right lateral bending (101%, $p = 0.035$).

***2) Upper level adjacent to PSR construct (T9–10) ROM***

Compared to the intact condition, ROM after PSR instrumentation was slightly higher at the upper level adjacent to the PSR construct (T9–10) for all load directions except flexion (mean decrease of 28%); however, no statistically significant difference

**Table 1.** Range of motion in degrees, at 3 levels of interest

| Level of interest | Flexion | Extension | Left lateral bending | Right lateral bending | Left axial rotation | Right axial rotation | Compression |
|---|---|---|---|---|---|---|---|
| T10–11 (upper instrumented level) | | | | | | | |
| Intact | 1.10 ± 0.74 | -1.77 ± 1.05 | -0.65 ± 0.45 | 1.16 ± 1.06 | 1.65 ± 0.78 | -1.65 ± 1.09 | |
| PSR | 0.33 ± 0.19*,† | -0.04 ± 0.13 | -0.13 ± 0.10 | 0.17 ± 0.10 | 0.42 ± 0.19 | -0.50 ± 0.23 | -0.03 ± 0.11 |
| PSR+PEEK | 0.10 ± 0.05*,† | -0.08 ± 0.07*,† | 0.03 ± 0.11 | -0.01 ± 0.11*,† | 0.39 ± 0.24 | -0.51 ± 0.28 | 0.04 ± 0.13 |
| T9–10 (upper level adjacent to PSR construct) | | | | | | | |
| Intact | 0.81 ± 0.68 | -1.24 ± 0.65 | -0.74 ± 0.34 | 1.17 ± 0.92 | 1.21 ± 0.88 | -1.58 ± 0.56 | |
| PSR | 0.62 ± 0.34 | -1.35 ± 0.59 | -1.14 ± 0.41 | 1.48 ± 0.93 | 1.69 ± 0.43 | -1.75 ± 0.61 | -0.42 ± 0.84 |
| PSR+PEEK | -0.09 ± 0.10*,†,‡ | 0.06 ± 0.16*,†,‡ | -0.62 ± 0.29*,‡ | 0.54 ± 0.24*,‡ | 0.91 ± 0.48 | -1.20 ± 0.67 | -0.06 ± 0.14 |
| T5–6 (upper level adjacent to PEEK rod) | | | | | | | |
| Intact | 1.07 ± 0.59 | -1.69 ± 0.97 | -1.15 ± 0.85 | 1.84 ± 0.66 | 1.46 ± 0.75 | -1.61 ± 0.41 | |
| PSR | 0.77 ± 0.45 | -1.34 ± 0.86 | -1.38 ± 074 | 1.58 ± 1.09 | 1.48 ± 0.47 | -1.74 ± 0.62 | 0.57 ± 0.25 |
| PSR+PEEK | 0.63 ± 0.47*,† | -0.76 ± 0.69 | -1.34 ± 0.64 | 1.48 ± 1.10 | 0.89 ± 0.51 | -0.88 ± 0.50*,†,‡ | 0.42 ± 0.63 |

PSR, pedicle screws from T10 to S1 and S2 alar-iliac screws and cobalt-chrome rods from T10 to S2; PEEK, polyetheretherketone; PSR+PEEK, PSR + pedicle screws at T6 and additional PEEK rod from T10 to T6.
Note that the compression range of motion is sagittal plane rotation (positive values = flexion, negative values = extension).
*$p < 0.05$, statistically significant differences. †Relative to intact using 1-way repeated-measures analysis of variance. ‡Relative to PSR using 1-way repeated-measures analysis of variance.

**Table 2.** Summary of all p-values for ROM and strain: PSR versus PSR+PEEK

| Level and measurement | Flexion | Extension | Left lateral bending | Right lateral bending | Left axial rotation | Right axial rotation | Compression |
|---|---|---|---|---|---|---|---|
| T10–11 ROM | 0.32 | 0.94 | 0.06 | 0.66 | 0.475 | 0.12 | 0.31 |
| T9–10 ROM | 0.02* | 0.003* | 0.02* | 0.008* | 0.27 | 0.47 | 0.31 |
| T5–6 ROM | 0.36 | 0.15 | 0.93 | 0.45 | 0.35 | 0.04* | 0.49 |
| T9 left anterior column bone strain | 0.26 | 0.42 | 0.09 | 0.02* | 0.22 | 0.60 | 0.26 |
| T10 right screw bending moment | 0.52 | 0.20 | 0.08 | 0.08 | 0.03* | 0.53 | 0.46 |
| T10–11 right posterior rod strain | 0.56 | 0.24 | 0.06 | 0.002* | 0.02* | 0.001* | 0.001* |

ROM, range of motion; PSR, pedicle screws from T10 to S1 and S2 alar-iliac screws and cobalt-chrome rods from T10 to S2; PEEK, polyetheretherketone; PSR+PEEK, PSR+pedicle screws at T6 and additional PEEK rod from T10 to T6.
Statistical comparisons of ROM assessed using a 1-way repeated-measures analysis of variance; comparisons of screw bending moments and bone and rod strains were analyzed using paired t-tests.
*$p < 0.05$, statistically significant differences.

was observed ($p \geq 0.27$). After extending the construct with PEEK rods, compared to PSR, ROM decreased in all directions with statistically significant differences in flexion (115%, $p = 0.02$), extension (104%, $p = 0.003$), left lateral bending (46%, $p = 0.02$), and right lateral bending (63%, $p = 0.008$), compared to PSR. Compared to the intact condition, PSR+PEEK showed a significant decrease in flexion (111%, $p = 0.01$) and extension (105%, $p = 0.003$).

*3) New upper level adjacent to PEEK rod (T5–6) ROM*

At the upper level adjacent to the PEEK construct (T5–6), when compared to the intact condition, PSR decreased ROM for flexion, extension, and right lateral bending (mean decrease 21%), and increased ROM for left lateral bending and left and right axial rotation (mean increase 10%), but these differences were not statistically significant ($p \geq 0.15$). For the PSR+PEEK versus PSR only, ROM decreased in all directions (mean 27%) but only significantly during right axial rotation (40%, $p = 0.04$). Compared to the intact condition, PSR+PEEK significantly decreased ROM during flexion (41%, $p = 0.048$) and right axial rotation (45%, $p = 0.044$).


https://doi.org/10.14245/ns.2244146.073

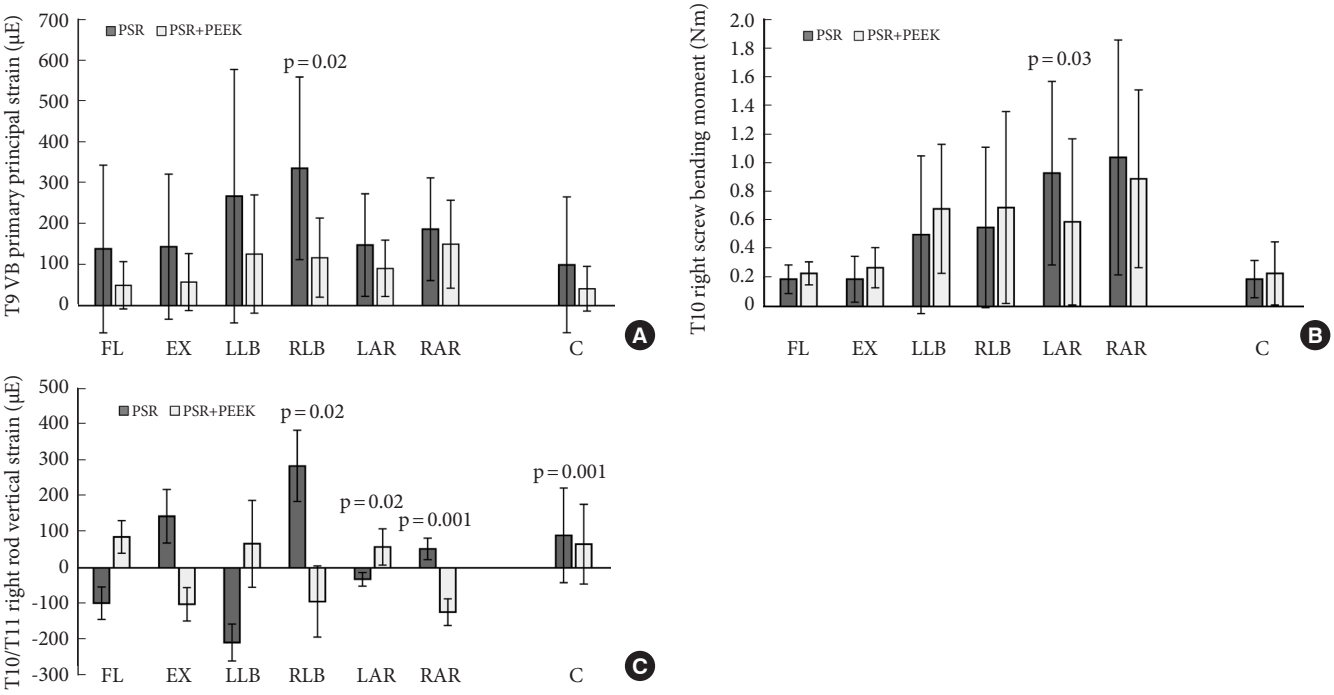


**Fig. 4.** Comparison of mean strain for PSR versus PSR+PEEK test conditions. (A) T9 anterior column bone primary principal strains (left anterolateral side). Note the reduced mean primary principal strains with PSR+PEEK versus PSR only, with the greatest reductions during lateral bending (significantly reduced during right lateral bending, p = 0.02). (B) Right screw bending moment. (C) Posterior right-side T10–11 rod strain. Error bars indicate standard deviation. PSR, pedicle screws from T10 to S1 and S2 alar-iliac screws and cobalt-chrome rods from T10 to S2; PEEK, polyetheretherketone; PSR+PEEK, PSR+pedicle screws at T6 and additional PEEK rod from T10 to T6; VB, vertebral body; FL, flexion; EX, extension; LLB, left lateral bending; RLB, right lateral bending; LAR, left axial rotation; RAR, right axial rotation; C, compression. Adapted with permission from Barrow Neurological Institute, Phoenix, Arizona.

**2. Strain**

All p-values for strain comparing PSR and PSR+PEEK conditions are summarized in Table 2, and comparisons of mean (SD) for PSR versus PSR+PEEK conditions are shown in Fig. 4.

*1) T9 anterior column bone strains*

Despite a large variability among specimens in terms of T9 anterior column bony surface strain, extending the PSR instrumentation above T9 with PEEK rods reduced the mean primary principal strain in most directions of motion in comparison to the PSR condition, with a statistically significant reduction during right lateral bending (p = 0.02) (Fig. 4A). (Note that no pedicle screws were inserted at this level.)

*2) T10 right pedicle screw bending moments*

Compared to the PSR condition, the addition of the PEEK rods caused a slight increase in mean T10 screw bending moment during bending in flexion (21%), extension (43%), right lateral bending (25%), left lateral bending (36%), and compression (24%), but these differences were not statistically significant (p ≥ 0.07). During axial rotation, added PEEK rods significantly reduced the mean right-side T10 screw bending moment by 37% during left axial rotation (contralateral side, p = 0.03); during right axial rotation, the bending moment decreased by 14%, which was not significant (ipsilateral side, p = 0.53) (Fig. 4B).

*3) T10-11 right-side posterior surface rod strains*

Compared to PSR alone, the addition of PEEK rods significantly decreased rod strain at T10–11 by 67% (188.8 μE, p = 0.002) in right lateral bending and by 27% (24.5 μE, p = 0.001) in compression, and it significantly increased strain by 83% (26.2 μE, p = 0.02) in left axial rotation and by 134% (70.3 μE, p = 0.001) in right axial rotation. Rod strain from the posterior side of the right rod between T10 and T11 shows that the direction of bending was reversed with PSR+PEEK versus PSR during all directions of loading (Fig. 4C). That is, local rod bending between T10 and T11 screws switched polarity from flexural rod strain

to an extension strain or vice versa with PSR+PEEK rods, except during compression when a flexural strain was maintained (Fig. 4C).

## DISCUSSION

The incidence of PJK after spinal fusion ranges from 17% to 62%.[19,20] PJK was defined by Glattes et al.[21] as a proximal junctional sagittal Cobb angle between the lower endplate of the UIV and the upper endplate of the 2 supra-adjacent vertebrae of ≥ 10° or at least 10° greater than the preoperative measurement; other authors have suggested 20° as the cutoff.[22,23] Currently, the term PJK has much broader connotations and includes different degrees of severity; however, an angulation of at least 10° greater than the preoperative angle is the most accepted definition of PJK.[24,25] Fracture at the UIV and screw loosening are the most common consequences. Risk factors include violation of posterior soft elements[26] (i.e., facet joint capsules, posterior tension band), large intraoperative curvature correction (> 30°), stiffness of the constructs, extension of the fusion, choice of the UIV, preexisting osteoporosis, older age (> 55 years), and high body mass index.[1] Because the stiffness of the construct is implicated in the development of PJK,[27,28] several prophylactic strategies have been discussed.[5-11] The biomechanical concept of using a semirigid bridge as a transition from a rigid to a flexible nonfused zone was addressed in this study, using PEEK rods attached to the proximal end of the PSR construct with inline connectors.

Using finite element analysis of long-segment spinal fusion, Yagi et al.[29] observed compressive stresses concentrated on the anterior column at both the UIV and adjacent level compared to intact spine. The strain measured on the anterolateral bone surface at UIV+1 (T9) in our study indicated a decrease in strain after extending the construct upward with PEEK rods. This finding potentially supports the hypothesis that the described technique can protect the anterior column from damaging shifts in mechanical stress involved with PJK genesis.

The choice for the cadaveric specimens and construct designs in the current study was made based on the attempt to approximate the physiological scenario but maximize the sensibility given the risk factors. We believe that our study is the first to demonstrate this result in cadavers and, more specifically, with long-segment constructs to the pelvis in specimens with the entire rib cage structure preserved. To the best of our knowledge, this study is the first T10-pelvis construct reproduced using cadavers with intact ribs in a biomechanical laboratory. Bridwell et al.[22] hypothesized that a stiffer construct may increase the risk of PJK. The choice of UIV at T10 in our study is supported by Bridwell et al.,[22] who reported that a UIV lower than T8 could increase the incidence of PJK. Previous clinical studies have shown that fusion to the sacrum and/or the ilium is also a significant risk factor.[30-33] A study by Kim et al.[34] supports the theory that distal spinal stability may be related to proximal stress via a relationship between iliac screw loosening and PJK. Preservation of the rib cage in the current study sought to mimic the physiological scenario because the rib cage has a stabilizing effect.[35,36]

In the present study, upper adjacent-level (T9–10) motion slightly increased after PSR, but not significantly. Extending the construct up to T6 with PEEK rods significantly decreased motion at this level in all directions compared to PSR. The effects of this decreased motion were noted in terms of decreased strain (i.e., stress) across the anterior column at T9 as well, with PEEK rods significantly decreasing left-side anterior column strain compared to PSR alone during right lateral bending ($p = 0.02$). The motion of the upper instrumented level (T10–11) decreased after PSR, with further increased rigidity achieved by the addition of PEEK rods. Ponnappan et al.[14] demonstrated *in vitro* that PEEK rods offer stability comparable to titanium rods (both 5.5-mm diameter) for lumbar fusion at the index level (not adjacent); however, the angular displacement achieved without failure was also in excess of that expected for normal nonfused physiologic lumbar motion.[37] Following PEEK rod extension in our specimens, the motion of the new adjacent level (T5–6) was significantly reduced in right axial rotation compared to PSR, unlike the "old adjacent level" (T9–10). This last finding may be important as it corroborates the hypothesis that the strategy studied has the potential to mitigate PJK because the motion is reduced and not increased at the new, more cranial adjacent level.

The addition of PEEK rods caused small to moderate increases in T10 screw bending moments in the sagittal plane, lateral bending, and in compression but did not reach statistical significance. Overall, and despite a statistically significant decrease in screw bending moments with PEEK compared to PSR during left axial rotation, no substantial differences in magnitudes were noticed. Changes with screw strains may be explained by the cantilever effect of bending loads applied to PEEK rods and transferred via the inline connector attached to the top of the titanium rod directly above the T10 screw. This connector receives and shares loads from spinal levels above (T6 to T9) spanning the PEEK rod stabilization. It may be hypothesized that if


https://doi.org/10.14245/ns.2244146.073

the extended UIV level were caudal to T6, this effect might be attenuated, especially given that there was no anchorage point between T10 and T6 in the PEEK condition.

Similar to T10 screw bending moments, PEEK rod extensions did not produce significant changes in T10–11 rod strain magnitudes in flexion and extension. PEEK rod extensions, however, significantly reduced rod strain in right lateral bending compared to PSR (the highest PSR rod strain magnitudes were noted in this direction) and significantly increased the smallest rod strains observed in the PSR condition in axial rotation. Rod strain polarities were also reversed with PEEK rods in all directions of loading except compression. With right lateral bending, for example, we might reasonably expect a caudally directed right-side force to bend the T10 screw and attached posterior rod into flexion. This effect would tend to induce a tensile strain on the posterior rod surface, as was observed. With attachment of the PEEK rod extensions, this mechanism was altered. Because it is well known that higher rod strains (and hence stress) directly correlate to reduced rod fatigue life and rod failure, in theory, strain magnitude reductions should result in a reduction in clinical instrumentation failure.

The notable observation in the current study of reversed T10–11 rod strain polarity with PEEK rod extension was also evident in changes in T9–10 flexion-extension ROM for the same condition. The rationale for this is unclear; however, several factors, including presence of the rib cage, the extended long length of the instrumented specimens, and a transitional region between thoracic and lumbar curvature, may have played a role. Notably the caudal PEEK rod attachment was located at or near the inflection point of these 2 curvatures. The concave and kyphotic curvature of the extension may have thus acted to influence directionality of cranially applied loads. The clinical significance of reversed strain polarity remains unclear.

The disruption of facet joint capsules and paraspinal musculature during open surgery approaches have been discussed as a potential risk factor for the development of PJK via the weakening of the soft tissue posterior tension band.[38] The strategy investigated in this study of extending the construct using PEEK rods can be performed through a minimally invasive approach and thus also has the potential to preserve these elements. This potential advantage was not addressed in the current study, and therefore further clinical studies are necessary.

The cadaveric biomechanics testing paradigm is a limitation of this study in that it only evaluates immediate stability. Further limitations include the absence of paraspinal and trunk muscles that play a role in stabilizing the spine and the absence of a targeted disease mechanism that represents an indication for the surgery. Our analysis of rod strain was localized and may not be reflective of overall strain distributions. Different types of distal ends in long-segment constructs commonly used in a clinical scenario might have affected the proximal junction differently (i.e., use of anterior column support at the base with interbody devices on L5–S1, use of multirod configurations, as well as stopping the construct at the sacrum and not extending to sacropelvic fixation). Strain gauge application near the head of the T6 screw required the screw head and neck region to extend substantially outside the pedicle. When combined with the fixed curvature of the PEEK rods, which cannot be bent to accommodate individual specimens, this construct was not practically viable in the cadaver anatomy and hence strain gauged T6 screws were not used. Following testing of the selected construct, other PEEK rod lengths were also practically difficult to implement in the same set of cadavers due to facet joint violation effects. The lack of other similar techniques for comparison is also acknowledged as a limitation of the present study. PJK is a multifactorial complication. Other loading scenarios not tested in the current study, as well as changing internal mechanical stresses that are not currently measurable, may be present.[39] Factors related to sagittal malalignment, miscorrection or overcorrection are also part of the PJK pathogenesis.[40] Cyclical loading was not included in the current study design as we believe that nondestructive load magnitudes used in standard biomechanical tests, coupled with tissue degeneration outside of the body, preclude any meaningful measure or simulation of prolonged *in vivo* service.

## CONCLUSION

Extending a long-segment construct using PEEK rods with connectors redistributed the strain on the upper instrumented and adjacent levels and caused a decrease in adjacent-level hypermobility that might be a contributing factor to the physiopathology of PJK. Additionally, this technique decreased the strain measured at the upper adjacent-level anterior column with, however, the trade-off of mildly increased proximal screw bending moment. Further studies are necessary to understand the biomechanical clinical outcomes of this technique.

## NOTES

**Conflict of Interest:** Juan S. Uribe receives consulting fees and royalties from NuVasive Medical, Inc., and is a consultant

for Masonix, Inc., and SI-BONE, Inc. Jay D. Turner is a consultant for NuVasive, SeaSpine, and AlphaTec. No other potential conflict of interest relevant to this article was reported.

**Funding/Support:** This study received no specific grant from any funding agency in the public, commercial, or not-for-profit sectors.

**Acknowledgments:** We gratefully acknowledge the donation of all spinal instrumentation used in the study by Medtronic plc. We thank the staff of Neuroscience Publications at Barrow Neurological Institute for assistance with manuscript preparation.

**Author Contribution:** Conceptualization: BDAP, JG, DX, JT, BK, JU; Data curation: BDAP, JL, AS, PW; Formal analysis: JL, AS; Funding acquisition: JU; Methodology: BDAP, BK, JU; Project administration: BK; Writing - original draft: BDAP; Writing - review & editing: BDAP, JT, BK, JU

**ORCID**

Bernardo de Andrada Pereira: 0000-0002-3990-9057
Jennifer N. Lehrman: 0000-0002-4364-8072
Anna G. U. Sawa: 0000-0003-3932-6668
Piyanat Wangsawatwong: 0000-0001-5797-7179
Jakub Godzik: 0000-0003-0645-6212
David S. Xu: 0000-0001-8987-4545
Jay D. Turner: 0000-0001-6867-3568
Brian P. Kelly: 0000-0002-5551-2834
Juan S. Uribe: 0000-0002-8910-6578

## REFERENCES

1. Hyun SJ, Lee BH, Park JH, et al. Proximal junctional kyphosis and proximal junctional failure following adult spinal deformity surgery. Korean J Spine 2017;14:126-32.
2. Glassman SD, Dimar JR 2nd, Carreon LY. Revision rate after adult deformity surgery. Spine Deform 2015;3:199-203.
3. Selim A, Mercer S, Tang F. Polyetheretherketone (PEEK) rods for lumbar fusion: a systematic review and meta-analysis. Int J Spine Surg 2018;12:190-200.
4. Abode-Iyamah K, Kim SB, Grosland N, et al. Spinal motion and intradiscal pressure measurements before and after lumbar spine instrumentation with titanium or PEEK rods. J Clin Neurosci 2014;21:651-5.
5. Mar DE, Clary SJ, Burton DC, et al. Biomechanics of prophylactic tethering for proximal junctional kyphosis: characterization of spinous process tether pretensioning and pull-out force. Spine Deform 2019;7:191-6.
6. Kebaish KM, Martin CT, O'Brien JR, et al. Use of vertebroplasty to prevent proximal junctional fractures in adult deformity surgery: a biomechanical cadaveric study. Spine J 2013;13:1897-903.
7. Martin CT, Skolasky RL, Mohamed AS, et al. Preliminary results of the effect of prophylactic vertebroplasty on the incidence of proximal junctional complications after posterior spinal fusion to the low thoracic spine. Spine Deform 2013;1:132-8.
8. Raman T, Miller E, Martin CT, et al. The effect of prophylactic vertebroplasty on the incidence of proximal junctional kyphosis and proximal junctional failure following posterior spinal fusion in adult spinal deformity: a 5-year follow-up study. Spine J 2017;17:1489-98.
9. Safaee MM, Deviren V, Dalle Ore C, et al. Ligament augmentation for prevention of proximal junctional kyphosis and proximal junctional failure in adult spinal deformity. J Neurosurg Spine 2018;28:512-9.
10. Han S, Hyun SJ, Kim KJ, et al. Effect of vertebroplasty at the upper instrumented vertebra and upper instrumented vertebra +1 for prevention of proximal junctional failure in adult spinal deformity surgery: a comparative matched-cohort study. World Neurosurg 2019 Jan 3;S1878-8750(18)32936-X. https://doi.org/10.1016/j.wneu.2018.12.113. [Epub].
11. Rodnoi P, Le H, Hiatt L, et al. Ligament augmentation with mersilene tape reduces the rates of proximal junctional kyphosis and failure in adult spinal deformity. Neurospine 2021;18:580-6.
12. Highsmith JM, Tumialan LM, Rodts GE Jr. Flexible rods and the case for dynamic stabilization. Neurosurg Focus 2007;22:E11.
13. Kurtz SM, Devine JN. PEEK biomaterials in trauma, orthopedic, and spinal implants. Biomaterials 2007;28:4845-69.
14. Ponnappan RK, Serhan H, Zarda B, et al. Biomechanical evaluation and comparison of polyetheretherketone rod system to traditional titanium rod fixation. Spine J 2009;9:263-7.
15. Bylski-Austrow DI, Glos DL, Bonifas AC, et al. Flexible growing rods: a biomechanical pilot study of polymer rod constructs in the stability of skeletally immature spines. Scoliosis Spinal Disord 2016;11:39.
16. Kelly BP, Bennett CR. Design and validation of a novel Cartesian biomechanical testing system with coordinated 6DOF real-time load control: application to the lumbar spine (L1-S, L4-L5). J Biomech 2013;46:1948-54.
17. Crawford NR, Dickman CA. Construction of local vertebral coordinate systems using a digitizing probe. Technical note.

Spine 1997;22:559-63.
18. Freeman AL, Fahim MS, Bechtold JE. Validation of an improved method to calculate the orientation and magnitude of pedicle screw bending moments. J Biomech Eng 2012; 134:104502.
19. Liu FY, Wang T, Yang SD, et al. Incidence and risk factors for proximal junctional kyphosis: a meta-analysis. Eur Spine J 2016;25:2376-83.
20. Kim HJ, Lenke LG, Shaffrey CI, et al. Proximal junctional kyphosis as a distinct form of adjacent segment pathology after spinal deformity surgery: a systematic review. Spine (Phila Pa 1976) 2012;37:S144-64.
21. Glattes RC, Bridwell KH, Lenke LG, et al. Proximal junctional kyphosis in adult spinal deformity following long instrumented posterior spinal fusion: incidence, outcomes, and risk factor analysis. Spine (Phila Pa 1976) 2005;30:1643-9.
22. Bridwell KH, Lenke LG, Cho SK, et al. Proximal junctional kyphosis in primary adult deformity surgery: evaluation of 20 degrees as a critical angle. Neurosurgery 2013;72:899-906.
23. O'Shaughnessy BA, Bridwell KH, Lenke LG, et al. Does a long-fusion "T3-sacrum" portend a worse outcome than a short-fusion "T10-sacrum" in primary surgery for adult scoliosis? Spine (Phila Pa 1976) 2012;37:884-90.
24. Cho SK, Shin JI, Kim YJ. Proximal junctional kyphosis following adult spinal deformity surgery. Eur Spine J 2014;23: 2726-36.
25. Hart RA, McCarthy I, Ames CP, et al. Proximal junctional kyphosis and proximal junctional failure. Neurosurg Clin N Am 2013;24:213-8.
26. Park PJ, Lombardi JM, Lenke LG. The Hybrid open muscle-sparing approach in adult spinal deformity patients undergoing lower thoracic fusion to the pelvis. Neurospine 2021; 18:234-9.
27. Han S, Hyun SJ, Kim KJ, et al. Rod stiffness as a risk factor of proximal junctional kyphosis after adult spinal deformity surgery: comparative study between cobalt chrome multiple-rod constructs and titanium alloy two-rod constructs. Spine J 2017;17:962-8.
28. Wui SH, Hyun SJ, Kang B, et al. Bicortical screw purchase at upper instrumented vertebra (UIV) can cause UIV fracture after adult spinal deformity surgery: a finite element analysis study. Neurospine 2020;17:377-83.
29. Yagi M, Nakahira Y, Watanabe K, et al. The effect of posterior tethers on the biomechanics of proximal junctional kyphosis: the whole human finite element model analysis. Sci Rep 2020;10:3433.
30. McClendon J Jr, Smith TR, Sugrue PA, et al. Spinal implant density and postoperative lumbar lordosis as predictors for the development of proximal junctional kyphosis in adult spinal deformity. World Neurosurg 2016;95:419-24.
31. Wang H, Ma L, Yang D, et al. Incidence and risk factors for the progression of proximal junctional kyphosis in degenerative lumbar scoliosis following long instrumented posterior spinal fusion. Medicine (Baltimore) 2016;95:e4443.
32. Yan P, Bao H, Qiu Y, et al. Mismatch between proximal rod contouring and proximal junctional angle: a predisposed risk factor for proximal junctional kyphosis in degenerative scoliosis. Spine (Phila Pa 1976) 2017;42:E280-7.
33. Kim JS, Phan K, Cheung ZB, et al. Surgical, radiographic, and patient-related risk factors for proximal junctional kyphosis: a meta-analysis. Global Spine J 2019;9:32-40.
34. Kim YH, Ha KY, Chang DG, et al. Relationship between iliac screw loosening and proximal junctional kyphosis after long thoracolumbar instrumented fusion for adult spinal deformity. Eur Spine J 2020;29:1371-8.
35. Liebsch C, Graf N, Appelt K, et al. The rib cage stabilizes the human thoracic spine: an in vitro study using stepwise reduction of rib cage structures. PLoS One 2017;12:e0178733.
36. Brasiliense LB, Lazaro BC, Reyes PM, et al. Biomechanical contribution of the rib cage to thoracic stability. Spine (Phila Pa 1976) 2011;36:E1686-93.
37. Panjabi MM, Krag MH, White AA 3rd, et al. Effects of preload on load displacement curves of the lumbar spine. Orthop Clin North Am 1977;8:181-92.
38. Denis F, Sun EC, Winter RB. Incidence and risk factors for proximal and distal junctional kyphosis following surgical treatment for Scheuermann kyphosis: minimum five-year follow-up. Spine (Phila Pa 1976) 2009;34:E729-34.
39. de Andrada Pereira B, Sawa AGU, Godzik J, et al. Influence of lumbar lordosis on posterior rod strain in long-segment construct during biomechanical loading: a cadaveric study. Neurospine 2021;18:635-43.
40. Pizones J, Moreno-Manzanaro L, Sanchez Perez-Grueso FJ, et al. Restoring the ideal Roussouly sagittal profile in adult scoliosis surgery decreases the risk of mechanical complications. Eur Spine J 2020;29:54-62.